Supplementary Material for Hofmann et al. (2017), EPSL

Evidence of >5 Ma paleo-exposure of an Eocene-Miocene paleosol of the Bohnerz Formation, Switzerland

Appendix A. ^{4}He/^{3}He experiments

The He-retention of a phase can be determined by measuring the natural distribution of ^{4}He by step-heating of samples with a uniform, proton-induced ^{3}He concentration (Shuster et al., 2003). Sample masses between 3 mg and 40 mg were picked from crushed pisoliths. They were irradiated on January 24th, 2015, with a 228.5 MeV proton beam with a fluence of $1.05 \cdot 10^{16}$ protons/cm^2 at the Francis H. Burr Proton Therapy Center at Massachusetts General Hospital for 5.5 hours to produce a uniform concentration of ^{3}He. The procedure follows the one described in Shuster et al. (2003). After irradiation the samples were stored for several months before analysis.

Appendix A.1. Pisoliths

Several pieces with a total mass between 0.4 and 1.2 mg were picked from irradiated sample material. They were enclosed in a copper packet and mounted on a thermocouple wire inside a diffusion cell. The samples were subjected to step-wise heating with a projector lamp (Farley et al., 1999) with 5-20°C steps between 25°C and 360°C and a heating time of 30 min per step. The temperature was within 2°C of the set temperature for steps 200°C, with a maximum overshoot of 10°C at temperatures over 300°C. The resulting gas was analyzed for ^{4}He and ^{3}He according to the procedure described in section Appendix B below.

The ^{4}He/^{3}He ratio of each step was normalized by the bulk ^{4}He/^{3}He ratio

and plotted against the cumulative fraction of ^{3}He released. The shape of this spectrum provides information about the spatial distribution of ^{4}He (Shuster et al., 2003; Shuster and Farley, 2003). No loss would be represented by a flat spectrum at unity. Any helium loss would lead to a deficit of ^{4}He in low-temperature steps.

^{4}He/^{3}He spectra were obtained for five different irradiated samples of pisolith cortices (Tab. A.1-A.3). The ^{4}He/^{3}He ratio is initially zero as ^{3}He is released at very low temperature steps (<50°C) and ^{4}He is below the detection limit. The normalized ^{4}He/^{3}He ratio then increases in the temperature steps over 50°C and approaches unity around 100°C. Most of the gas was released between 90°C and 120°C. The shape of the ^{4}He/^{3}He spectra are consistent with isothermal accumulation and diffusion (Shuster and Farley, 2003; Shuster et al., 2003). The resulting retention is between 93% and 98% (Figs. A.1-A.3).

All ages and concentrations given here are uncorrected for partial He retentivity. Since the retentivities that were obtained using the ^{4}He/^{3}He method are between 93% and 98%, (U-Th)/He ages as well as ^{3}He concentrations may be up to 7% higher than stated here.

FH-F1-BR01-irr (0.41 mg)						FH-F2-BR04-irr (0.61)					
Step Number	Temp. [°C]	^{3}He [pcc]	$\pm1\sigma$ [pcc]	^{4}He [ncc]	$\pm1\sigma$ [ncc]	Step Number	Temp. [°C]	^{3}He [pcc]	$\pm1\sigma$ [pcc]	^{4}He [ncc]	$\pm1\sigma$ [ncc]
0	25	bdl		bdl		0	25	bdl		bdl	
1	40	0.0468	0.0004	bdl		1	50	0.2667	0.0012	bdl	
2	60	0.2927	0.0015	bdl		2	70	0.8342	0.0027	bdl	
3	80	0.1754	0.0010	bdl		3	80	0.7111	0.0021	0.1950	0.0044
4	85	0.4247	0.0017	0.0419	0.0056	4	90	2.8084	0.0064	1.7476	0.0040
5	90	0.3633	0.0014	0.1622	0.0038	5	95	3.6331	0.0088	2.3587	0.0037
6	95	0.5773	0.0017	0.3808	0.0042	6	100	1.3519	0.0040	0.9117	0.0049
7	100	1.7300	0.0036	1.3702	0.0046	7	105	0.3091	0.0016	0.1925	0.0016
8	110	6.2340	0.0096	5.4089	0.0056	8	110	1.0308	0.0036	0.6009	0.0036
9	120	1.9289	0.0060	1.8235	0.0061	9	115	4.8058	0.0084	2.9342	0.0034
10	130	0.0700	0.0007	0.0595	0.0030	10	120	1.6365	0.0036	1.0077	0.0062
11	140	0.1317	0.0012	0.1128	0.0041	11	130	0.7457	0.0022	0.4542	0.0036
12	160	0.3136	0.0011	0.2941	0.0042	12	140	0.0621	0.0007	bdl	
13	180	1.3017	0.0030	1.1682	0.0040	13	160	1.1415	0.0030	0.8077	0.0036
14	200	0.3807	0.0016	0.3421	0.0021	14	180	0.3428	0.0017	0.2335	0.0020
15	220	0.3691	0.0021	0.3458	0.0025	15	200	0.5312	0.0018	0.3360	0.0063
16	240	0.1795	0.0010	0.1624	0.0038	16	220	0.6418	0.0024	0.4235	0.0038
17	260	0.2595	0.0014	0.2232	0.0038	17	240	0.2050	0.0011	0.1214	0.0038
18	280	0.1718	0.0010	0.1650	0.0043	18	260	0.3052	0.0011	0.1961	0.0053
19	300	0.0658	0.0007	0.0657	0.0046	19	280	0.3884	0.0016	0.2808	0.0030
20	320	0.0553	0.0006	0.0439	0.0050	20	300	0.0534	0.0005	bdl	
21	340	0.0479	0.0004	0.0451	0.0042	21	320	0.0456	0.0005	bdl	
22	360	0.0339	0.0003	bdl		22	340	0.0436	0.0008	bdl	

Table A.1: Results of the ^{4}He/^{3}He experiment of samples FH-F1-BR01-irr and FH-F2-BR04-irr from pisolith cortices. Aliquots were degassed for 30 min at each step (bdl = below detection limit).

FH-F3-BR03-3rdlayer-irr3 (0.46 mg)						FH-F4-BR05-4thlayer-irr4 (0.36 mg)					
Step Number	**Temp. [°C]**	**^{3}He [pcc]**	**$\pm1\sigma$ [pcc]**	**^{4}He [ncc]**	**$\pm1\sigma$ [ncc]**	**Step Number**	**Temp. [°C]**	**^{3}He [pcc]**	**$\pm1\sigma$ [pcc]**	**^{4}He [ncc]**	**$\pm1\sigma$ [ncc]**
0	25	bdl		bdl		0	30	bdl		bdl	
1	40	0.0199	0.0003	bdl		1	40	0.0023	0.0001	bdl	
2	60	0.2492	0.0012	bdl		2	60	0.0348	0.0004	bdl	
3	80	0.6312	0.0021	0.1134	0.0018	3	80	0.0842	0.0006	bdl	
4	90	5.8018	0.0098	4.7860	0.0048	4	90	0.1967	0.0010	0.0795	0.0029
5	100	5.3090	0.0110	4.8500	0.0050	5	100	2.0933	0.0052	1.5022	0.0050
6	110	2.4622	0.0063	2.3401	0.0052	6	110	1.7465	0.0038	1.2821	0.0015
7	120	0.0532	0.0006	bdl		7	120	1.7356	0.0086	1.2963	0.0058
8	130	0.0313	0.0002	bdl		8	130	0.1288	0.0009	0.0955	0.0055
9	140	0.1831	0.0010	0.1656	0.0049	9	140	0.6805	0.0028	0.4796	0.0042
10	150	1.1564	0.0033	1.0613	0.0032	10	150	0.2915	0.0011	0.1823	0.0042
11	160	0.6346	0.0019	0.5831	0.0051	11	160	0.0784	0.0007	0.0592	0.0051
12	170	0.1707	0.0012	0.1665	0.0045	12	170	0.1132	0.0009	0.0774	0.0057
13	180	0.2136	0.0011	0.1875	0.0021	13	180	0.0614	0.0006	0.0424	0.0039
14	200	0.3968	0.0014	0.3683	0.0046	14	200	0.3280	0.0015	0.2323	0.0058
15	220	0.1703	0.0010	0.1566	0.0036	15	220	0.1051	0.0008	0.0822	0.0034
16	240	0.1406	0.0011	0.1528	0.0033	16	240	0.0958	0.0008	0.0721	0.0030
17	260	0.0814	0.0007	0.0866	0.0025	17	260	0.2449	0.0013	0.1747	0.0043
18	280	0.0724	0.0006	0.0606	0.0039	18	280	0.0721	0.0005	0.0581	0.0022
19	300	0.0198	0.0002	0.0168	0.0039	19	300	0.0094	0.0001	bdl	
20	320	0.0149	0.0003	bdl		20	320	0.0316	0.0004	bdl	
21	340	0.0116	0.0008	bdl		21	340	0.0210	0.0002	bdl	
22	360	0.0073	0.0001	bdl		22	360	0.0148	0.0003	bdl	

Table A.2: Results of the ^{4}He/^{3}He experiment of samples FH-F3-BR03-3rdlayer-irr3 and FH-F4-BR05-4thlayer-irr4 from different layers of the same pisolith cortex. Aliquots were degassed for 30 min at each step (bdl = below detection limit).

FH-F5-BR05-core-irr3 (0.41 mg)						FH-L120a-diff (56.44 mg)					
Step Number	**Temp. [°C]**	**^{3}He [pcc]**	**$\pm1\sigma$ [pcc]**	**^{4}He [ncc]**	**$\pm1\sigma$ [ncc]**	**Step Number**	**Temp. [°C]**	**^{3}He [pcc]**	**$\pm1\sigma$ [pcc]**	**^{4}He [ncc]**	**$\pm1\sigma$ [ncc]**
0	25	bdl		bdl		0	22	bdl		bdl	
1	40	0.0760	0.0004	bdl		1	40	0.0072	0.0002	bdl	
2	60	0.4036	0.0018	bdl		2	60	0.0013	0.0001	bdl	
3	80	1.2538	0.0057	0.2116	0.0049	3	80	0.0021	0.0001	0.0543	0.0048
4	90	0.9722	0.0040	0.4952	0.0038	4	100	0.0027	0.0002	1.0135	0.0019
5	100	3.6078	0.0086	2.1444	0.0014	5	120	0.0087	0.0002	10.3108	0.0057
6	110	5.5278	0.0096	3.4786	0.0038	6	160	0.0766	0.0008	107.3692	0.0541
7	120	6.0570	0.0198	4.0500	0.0030	7	199	0.2277	0.0020	343.3449	0.2551
8	130	0.3921	0.0020	0.2518	0.0032	8	239	0.2581	0.0018	435.7943	0.2654
9	140	0.0025	0.0001	bdl		9	274	0.0212	0.0003	42.4120	0.0125
10	150	0.0205	0.0002	bdl		10	276	0.0117	0.0004	19.7384	0.0238
11	160	1.0682	0.0039	0.7459	0.0046	11	294	0.0155	0.0002	34.9967	0.0239
12	170	0.5255	0.0018	0.3380	0.0029	12	313	0.0160	0.0004	32.6238	0.0140
13	180	0.3413	0.0016	0.2433	0.0047						
14	200	0.6308	0.0025	0.4463	0.0059						
15	220	0.1969	0.0013	0.1444	0.0015						
16	240	0.5091	0.0021	0.3538	0.0020						
17	260	0.0025	0.0002	bdl							
18	280	0.3272	0.0012	0.2354	0.0044						
19	300	0.0890	0.0007	0.0583	0.0024						
20	320	0.0744	0.0003	0.0511	0.0043						
21	340	0.0481	0.0005	bdl							
22	360	0.0423	0.0005	bdl							

Table A.3: Results of the ^{4}He/^{3}He experiment of samples FH-F5-BR05-core-irr3 from fine-grained material of the nucleus of pisolith BR05 and un-irradiated cortex material of pisolith FH-L120a-diff. Aliquots were degassed for 30 min at each step (bdl = below detection limit).

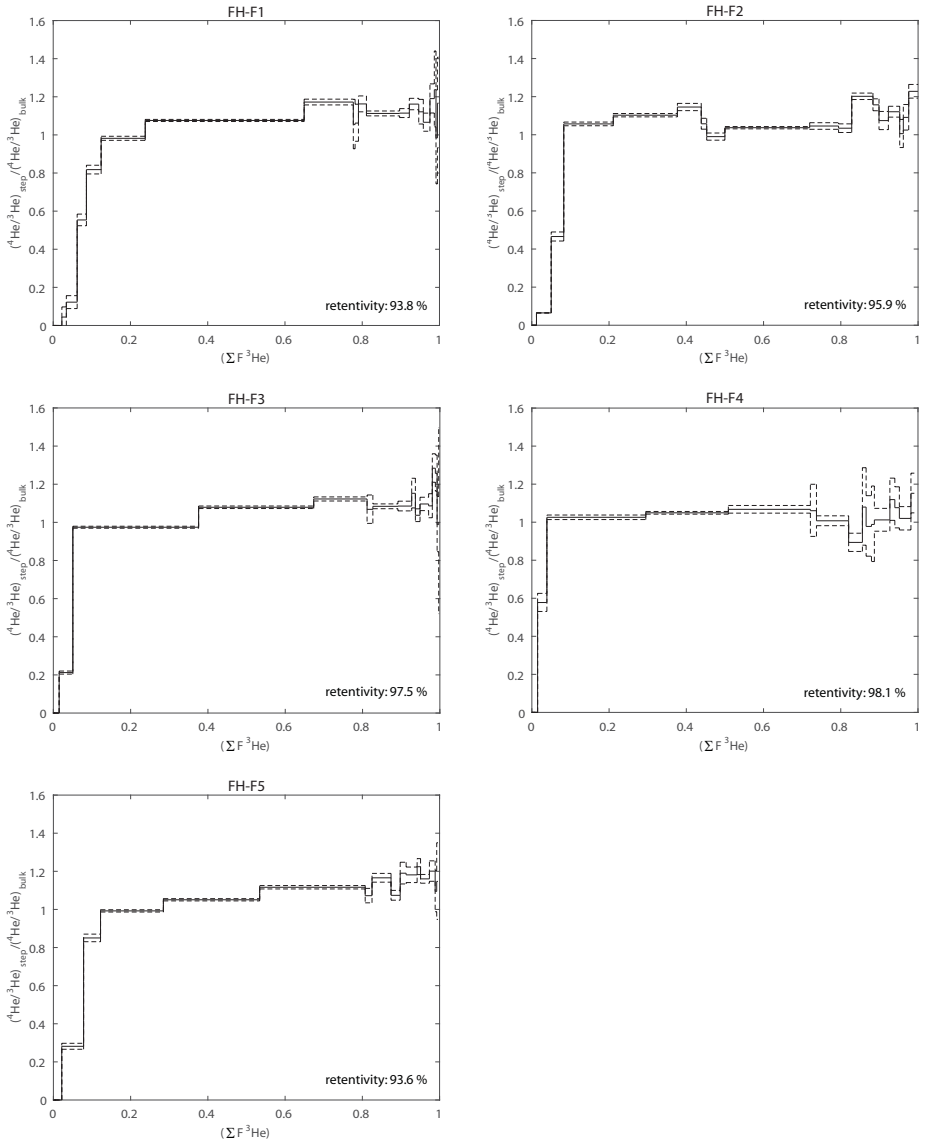

Figure A.5: Normalized ^{4}He/^{3}He spectra of samples FH-F1 through FH-F5. Samples FH-F1 and FH-F2 were taken from the cortex of two different pisoliths. Samples FH-F3, FH-F4, and FH-F5 were taken from the 3rd and 4th layer of the cortex as well as the finer-grained nucleus of the same pisolith. The dashed line shows the 1σ uncertainty of the ^{4}He/^{3}He ratio.

Appendix A.2. Un-irradiated Pisolith

In order to investigate whether the complex, poly-crystalline goethite of the pisoliths can trap ^{3}He from air, we performed a step-heating experiment of un-irradiated cortex material (Tab. A.3). Any helium from air, which is more loosely bound by surface adhesion than radiogenic helium, is expected be released at lower temperature steps. Since air has a higher ^{3}He/^{4}He ratio than radiogenic helium, ^{3}He would disproportionally be released at lower temperatures. Material from pisolith L120a was selected because it had previously yielded the highest ^{3}He concentration. This ensured that it contained enough ^{3}He to be above blank level when degassed in several temperature steps. The un-irradiated sample was prepared and analyzed as described above. The fraction released in every temperature step was the same for ^{3}He and ^{4}He within uncertainty (Fig. A.6). This shows that both ^{3}He and ^{4}He are equally strongly bound. The results of this experiment do not show a higher ^{3}He/^{4}He ratio in low temperature steps. This is consistent with uniformly distributed and strongly-bound ^{3}He from cosmogenic production and radiogenic ^{4}He.

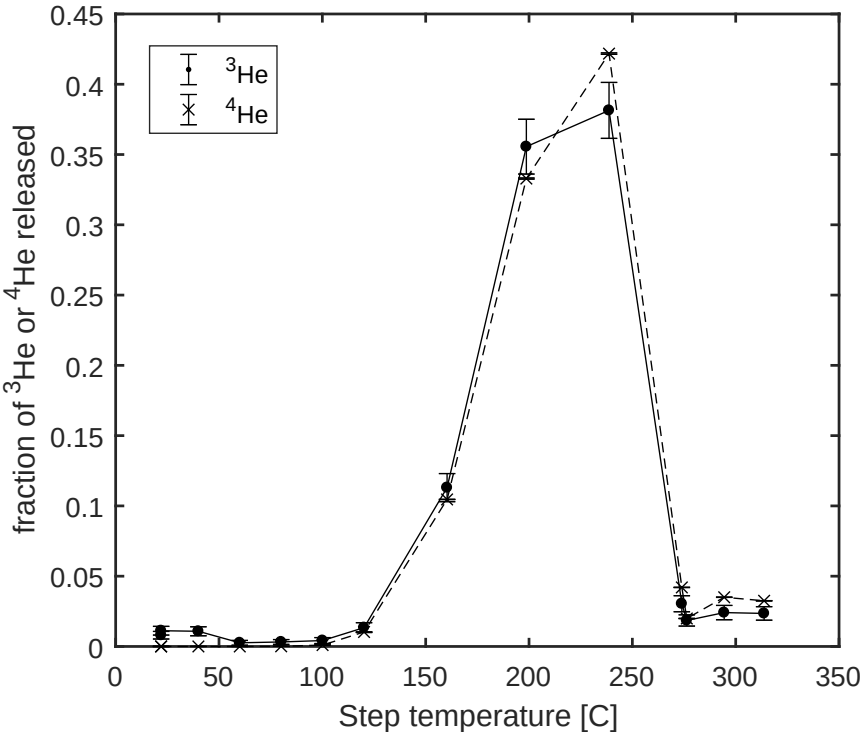

Figure A.6: Results of a step-heating experiment with un-irradiated goethite from cortex material of pisolith L120a. The relative amounts of ^{3}He and ^{4}He are the same for every temperature step, showing that both isotopes are equally strongly bound.

Appendix B. Concentrations of ^{3}He

Appendix B.1. Pisoliths

About 10-20 mg of goethite picked from crushate was weighed and wrapped in tin foil. Samples were de-gassed at 1300°C for 30 min in a double-vacuum resistance furnace. Re-extracts at 1350°C were performed after every sample to verify complete He extraction. The extracted gas was fed through a U-trap filled with activated charcoal and submerged in liquid nitrogen and then reacted with a SAES getter. The gas was fixed on a cryogenic trap at 14 K and then released into the MAP 215-50 magnetic sector field mass spectrometer at 34 K. The abundance of ^{3}He and ^{4}He was measured on an electron multiplier and Faraday cup, respectively. The sensitivity of the mass spectrometer was determined by gas standards with a known ^{3}He/^{4}He ratio of 2.01 RA. Different amounts of standard gas are used to establish linearity within the range of measurement. Analytical detection limits of ^{3}He and ^{4}He are around $1.7{\cdot}10^{-20}$ mol and $5.0{\cdot}10^{-15}$ mol, respectively. Interspersed standards and blanks throughout each experiment were used to correct for drift in sensitivity.

Sample Name	d [cm]	mass [mg]	$^3He/^4He$ 10^{-7}	^3He [amol]	$\pm 1\sigma$ [amol]	c(^3He) [Mat/g]	$\pm 1\sigma$ [Mat/g]
Lula2	ul	15.10	0.599	0.642	0.129	26	5
Lulb1	ul	12.45	12.730	10.296	0.460	498	22
Lulc2	ul	3.88	5.886	2.228	0.268	346	42
Luld1	ul	1.32	13.030	0.742	0.134	339	61
Lule1	ul	20.64	5.629	9.395	0.482	274	14
Lulf1	ul	1.36	10.430	0.703	0.107	311	47
L0a2	5	7.24	5.807	4.596	0.295	382	25
L0b1	5	10.44	7.741	9.159	0.451	528	26
L0c1	5	5.50	6.515	0.664	0.129	73	14
L0c2	5	7.04	3.661	0.860	0.161	74	14
L0d1	5	4.18	3.304	1.829	0.210	263	30
L0e1	5	7.41	5.368	3.518	0.295	286	24
L0f1	5	7.88	5.814	4.844	0.371	370	28
L10a1	15	26.68	6.529	17.733	0.598	400	14
L10b1	15	7.40	5.772	4.409	0.313	359	25
L10c1	15	10.78	6.515	5.728	0.393	320	22
L10c2	15	15.68	5.081	9.169	0.433	352	17
L10d1	15	8.61	6.206	5.383	0.371	377	26
L10e1	15	31.04	3.092	11.390	0.540	221	11
L20a1	23	28.53	3.413	17.509	0.612	370	13
L20a2	23	9.50	3.207	6.158	0.357	390	23
L20b1	23	4.75	4.286	1.972	0.219	250	28
L20c1	23	7.62	2.163	2.053	0.210	162	17
L20d2	23	6.59	3.946	4.507	0.330	412	30
L20e1	23	12.11	5.908	3.904	0.277	194	14
L30a1	33	10.70	2.917	1.759	0.188	99	11
L30b1	33	15.36	7.921	9.522	0.442	373	17
L30c1	33	6.62	5.030	3.010	0.281	274	26
L30d1	33	13.24	8.960	8.193	0.429	373	20
L30e1	33	14.93	4.034	6.055	0.379	244	15
L50a1	45	4.67	2.643	1.330	0.183	172	24
L50b1	45	25.27	4.417	11.841	0.442	282	11
L50c1	45	14.30	3.273	3.233	0.263	136	11
L50d1	45	23.00	3.825	10.145	0.438	266	12
L50e1	45	15.68	5.031	9.280	0.549	356	21
L70a2	60	14.28	0.709	0.933	0.125	39	5
L70a3	60	3.84	0.660	0.244	0.085	38	13
L70b1	60	20.51	3.509	8.532	0.455	251	13
L70c1	60	3.87	2.970	1.161	0.152	181	24
L70d1	60	12.94	3.051	4.109	0.254	191	12
L70e1	60	24.90	9.761	11.575	0.509	280	12
L80a1	75	6.50	3.481	3.676	0.290	341	27
L80a2	75	10.49	3.477	5.106	0.353	293	20

Table B.4: Measured ^{3}He concentration of pisolith cortices (mass = mass of aliquot, d = depth below freshwater limestone layer, c = concentration of ^{3}He per sample mass, ul = layer of paleosol above freshwater limestone).

Sample Name	d [cm]	mass [mg]	$^3He/^4He$ 10^{-7}	^3He [amol]	$\pm 1\sigma$ [amol]	c(^3He) [Mat/g]	$\pm 1\sigma$ [Mat/g]
L80b1	75	14.14	0.455	0.842	0.125	36	5
L80b2	75	11.12	0.475	0.648	0.112	35	6
L80c1	75	30.15	5.054	15.422	0.656	308	13
L80d1	75	18.59	5.368	8.721	0.442	283	14
L80e1	75	6.32	7.489	5.035	0.353	480	34
L90a2	87	42.58	5.683	13.757	0.585	195	8
L90b1	87	13.53	7.117	10.521	0.424	468	19
L90c1	87	21.60	5.380	12.066	0.589	336	16
L90d2	87	6.12	4.712	1.240	0.179	122	18
L90e1	87	9.15	3.592	2.696	0.241	177	16
L120a1	116	19.99	6.432	16.796	0.527	506	16
L120a2	116	13.99	6.738	14.233	0.563	613	24
L120a3	116	7.77	6.860	7.747	0.420	600	33
L120b1	116	26.33	6.500	17.972	0.665	411	15
L120c1	116	6.13	1.578	1.279	0.179	126	18
L120c2	116	5.89	1.824	1.197	0.147	122	15
L120d2	116	4.32	3.058	2.649	0.241	369	34
L120e1	116	10.12	5.698	10.486	0.473	624	28
L120f1	116	1.39	7.533	0.779	0.134	338	58
L120f2	116	0.48	7.224	0.275	0.085	345	106
L120f3	116	0.85	6.429	0.437	0.098	309	70
L120f4	116	1.61	6.097	0.869	0.152	325	57
L120f5	116	1.24	4.785	0.697	0.134	339	65
L120f6	116	0.42	4.660	0.263	0.089	378	128
L120f7	116	1.63	4.088	0.747	0.138	276	51
L120g1	116	6.75	2.918	1.965	0.219	175	20
L170a2	164	8.60	5.654	5.469	0.326	383	23
L170b1	164	34.33	9.969	19.597	0.621	344	11
L170c1	164	5.77	4.577	2.202	0.250	230	26
L170c2	164	9.40	6.149	4.529	0.348	290	22
L170d1	164	6.46	5.128	2.291	0.254	214	24
L170e1	164	2.70	6.774	1.019	0.138	227	31
L250a1	268	12.00	5.352	6.350	0.388	319	20
L250b1	268	5.09	5.384	2.261	0.210	268	25
L250c1	268	11.48	1.555	2.632	0.228	138	12
L250d2	268	5.61	3.339	2.262	0.250	243	27
L250e1	268	25.49	7.948	16.706	0.612	395	14
L300a1	339	15.02	2.579	2.937	0.223	118	9
L300a2	339	8.14	2.557	1.503	0.183	111	14
L300b1	339	18.10	4.915	9.546	0.451	318	15
L300b2	339	14.30	4.554	7.470	0.357	315	15
L300c1	339	2.25	5.193	0.843	0.152	226	41
L300c2	339	4.09	4.659	1.411	0.170	208	25
L300d1	339	26.35	3.888	6.057	0.366	138	8
L300e1	339	12.29	0.958	1.342	0.174	66	9
L300g1	339	5.48	4.743	1.899	0.241	209	27

Table B.5: Measured ^{3}He concentration of pisolith cortices continued.

Appendix B.2. Fine-grained iron-oxides in clay

About 10-150 mg of red clay from the paleosol was analyzed for ^{3}He as described above. An aliquot of about 2 mg of the same crushate was used for chemical analysis. Fine-grained Fe-oxides in the clay were dissolved with 200 µl of concentrated HCl at 95°C for 72 hours, leaving a kaolinite residue. The solutions were spiked and analyzed for Fe using isotope-dilution ICP-MS as described below in section Appendix C. The ^{3}He concentration was calculated based on the Fe-oxide fraction of the clay.

Sample Name	d [cm]	mass [mg]	^{3}He/^{4}He 10^{-7}	^{3}He [amol]	$\pm1\sigma$ [amol]	f_{gt}	c(^{3}He) Mat/g	$\pm1\sigma$ Mat/g
Lulclay1	ul	81.98	1.336	1.2188	0.1964	0.1897	47	8
Lulclay3	ul	26.33	3.400	1.3751	0.2188	0.1021	308	51
L0clay1	5	27.31	3.111	0.7813	0.1473	0.0605	285	56
L0clay3	5	59.82	2.828	1.9196	0.2277	0.0743	260	33
L20clay1	23	11.02	3.762	0.3705	0.0982	0.0774	262	71
L20clay3	23	12.86	3.060	0.5446	0.1339	0.0936	273	68
L20clay4	23	41.63	2.800	1.7232	0.2411	0.1188	210	31
L20clay5	23	53.77	9.135	2.9420	0.3348	0.1407	234	29
L30clay1	33	38.35	4.273	1.7679	0.2232	0.0824	337	46
L30clay3	33	13.39	2.652	0.5089	0.1339	0.1432	160	43
L50clay1	45	16.13	2.450	0.4598	0.1205	0.0876	196	52
L50clay3	45	40.07	1.803	1.7366	0.2545	0.0942	277	43
L70clay1	60	18.83	3.698	0.8125	0.1563	0.1468	177	35
L70clay3	60	26.87	2.772	1.0000	0.1607	0.1533	146	25
L80clay1	75	27.93	2.489	1.0670	0.1786	0.1605	143	25
L80clay3	75	87.86	3.786	4.1741	0.3527	0.1159	247	24
L90clay1	87	34.73	2.914	1.4018	0.2054	0.1469	165	26
L90clay3	87	47.29	3.076	1.6786	0.2545	0.1259	170	27
L120clay1	116	70.68	3.408	2.4509	0.2857	0.0834	250	32
L120clay3	116	23.28	2.931	0.8571	0.1696	0.1143	194	40
L170clay1	164	41.26	3.281	1.7143	0.2321	0.0819	306	44
L170clay3	164	16.84	3.197	0.5759	0.1295	0.1092	189	43
L170clay4	164	157.41	2.850	4.5625	0.3616	0.1531	114	11
L250clay1	268	23.67	3.763	1.5491	0.2009	0.0971	406	56
L250clay3	268	32.57	3.565	1.7321	0.2277	0.1355	236	33
L300clay1	339	14.53	2.005	0.5804	0.1339	0.1044	230	54
L300clay3	339	96.51	3.079	3.8750	0.3527	0.0986	245	25
L300clay4	339	43.23	2.903	1.8170	0.2188	0.1029	246	32

Table B.6: Results of ^{3}He concentration measurements of fine-grained iron-oxides in soil (d = depth below freshwater limestone layer, ul = layer of paleosol above freshwater limestone, mass = mass of the bulk soil sample degassed to measure ^{3}He, f_{gt} mass fraction of iron-oxides stoichiometrically calculated as goethite, c(^{3}He) = concentration of ^{3}He based on mass fraction of iron-oxides). Two different aliquots were used to measure ^{3}He bulk concentration and iron-oxide mass fraction. The ^{3}He concentration was calculated based on the amount of iron-oxide in the aliquot used for ^{3}He analysis.

Appendix B.3. Exposure modeling of soil convection

To estimate the exposure duration we modeled soil convection as a continuous circular motion throughout the whole thickness of the paleosol (3.6 m). This leads to a constant concentration profile of ^{3}He in the soil for any total exposure duration that is longer than the timescale of soil convection. Since the exposure duration here is at least several Ma, we find this to be a justifiable assumption. The cosmogenic ^{3}He production rate at the surface, scaled for latitude and a range in paleo-elevation, is between 79 and 129 atoms/g/a. The production rate decreases exponentially with depth (Lal, 1991). We assumed an attenuation length of 160 g cm^{-2} (Gosse and Phillips, 2001) and a density of 1.6 g·cm^{-3}. This yields an absorption coefficient of 0.01·cm^{-1}, which corresponds to an e-folding depth of 100 cm. At the base of the paleosol the production rate is <1% of the production rate at the surface. We numerically integrated the time any parcel spends at 3000 different depths between 0 and 360 cm on a circular trajectory. Since the resulting concentration is constant, the equivalent production rate is the same for every depth. To address uncertainties in the production rate, attenuation path length, and paleo-elevation we used a Monte-Carlo approach to propagate these uncertainties to the equivalent production rate. The equivalent production rate for this soil convection model is (33.9±5.4) atoms/g/a. For an average concentration of 300 Matoms/g, this corresponds to an exposure duration of (8.8±1.7) Ma.

Appendix C. Goethite (U-Th)/He ages

Several aliquots of the crushate of each pisolith were selected for age dating. Individual pieces with a cross-section of 100-500 µm and a mass of approximately 5-50 µg were loaded into platinum tubes. Samples in Pt tubes were heated to 900°C using a Photon Machines YAG laser and degassed under vacuum for 360 seconds. A pure ^{3}He spike for isotope dilution was added. The gas was cryogenically fixed at 14 K and released into the Pfeiffer Vacuum quadrupole mass spectrometer at 36 K. The sensitivity of the instrument was calibrated using a standard of known ^{4}He amount. Re-extracts at 950°C were performed for every sample to ensure complete He extraction.

After degassing the Pt packets were transferred to Teflon vials. For isotope dilution, 25 µl of spike with 12.04 ng/ml of ^{235}U and 21.37 ng/ml of ^{230}Th, and ^{232}Th/^{230}Th and ^{238}U/^{235}U ratios of 0.09 and 0.007, respectively, as well as 10000 ppm of Ca was added. Each aliquot was dissolved in 100 µl of concentrated Seastar™ HCl for 12 h at 95°C. The solution was dried down by heating to 95°C for 1 h. The precipitate was brought into solution with 50 µl of concentrated Seastar™ HNO_3. The solution was diluted with 1000 µl of Milli-Q® water. A spiked normal solution with known amounts U, Th, and Fe was prepared. The ^{238}U, ^{232}Th, and Fe content of the solutions as well as the composition of the spike and the normal solution were determined using an Agilent 7500 inductively coupled plasma quadrupole mass spectrometer (ICP-MS) as well as an Agilent 8800 triple-quadrupole ICP-MS.

We assumed zero initial ^{4}He, no diffusive loss or gain for He, U, and Th, as well as secular equilibrium among daughter nuclides of the ^{238}U, ^{235}U, and ^{232}Th decay series. The (U-Th)/He age was calculated according to Farley

(2002). Since the diameter of the pisoliths (1-50 mm) and the thickness of layers of equal age (at least 100-200 μm) is much larger than the α-stopping distance ($\sim$20 µm) of the U and Th series decays (Farley et al., 1996; Farley, 2002) no correction for α-implantation or α-ejection was applied.

Sample Name	d [cm]	age [Ma]	$\pm1\sigma$ [Ma]	U [ppm]	$\pm1\sigma$ [ppm]	Th [ppm]	$\pm1\sigma$ [ppm]	^{4}He [nmol/g]	$\pm1\sigma$ [nmol/g]	Gt Mass [μg]
FH-L-ul-a1	ul	27.45	1.22	3.93	0.15	26.39	0.59	1.521	0.008	7.39
FH-L-ul-b2	ul	17.89	0.75	1.91	0.07	28.68	0.50	0.851	0.008	13.67
FH-L-ul-c1	ul	18.25	0.54	4.46	0.12	39.79	0.53	1.372	0.017	25.39
FH-L-ul-c2	ul	21.97	0.88	2.55	0.17	35.14	0.60	1.293	0.010	13.92
FH-L-ul-c3	ul	19.44	0.69	5.12	0.16	37.97	0.63	1.487	0.010	11.44
FH-L-ul-d1	ul	36.55	2.10	0.97	0.19	22.93	0.53	1.267	0.008	10.25
FH-L-ul-d3	ul	25.42	1.61	3.95	0.19	28.68	0.80	1.480	0.006	3.97
FH-L-ul-e1	ul	24.65	0.80	2.86	0.08	17.18	0.28	0.926	0.012	26.51
FH-L-ul-e2	ul	21.90	0.56	4.04	0.07	21.04	0.25	1.071	0.032	65.89
FH-L-ul-e3	ul	25.10	0.99	3.06	0.11	16.88	0.34	0.961	0.008	14.06
FH-L-0-a1	5	20.02	0.78	2.84	0.11	58.23	0.95	1.805	0.009	8.55
FH-L-0-a2	5	19.19	1.05	3.69	0.17	50.10	1.08	1.619	0.007	4.30
FH-L-0-a3	5	21.52	0.73	1.42	0.10	39.51	0.54	1.255	0.015	24.90
FH-L-0-b1	5	21.30	1.27	3.98	0.17	32.95	0.82	1.366	0.007	4.55
FH-L-0-b2	5	29.35	1.08	3.09	0.13	75.81	1.21	3.350	0.012	7.01
FH-L-0-b3	5	22.01	0.70	3.65	0.12	69.04	0.93	2.388	0.016	13.95
FH-L-0-d1	5	27.57	0.93	4.22	0.14	46.95	0.74	2.291	0.013	11.11
FH-L-0-d3	5	23.97	0.75	3.56	0.11	48.91	0.67	1.965	0.016	17.40
FH-L-0-e1	5	21.85	0.64	2.53	0.07	29.86	0.38	1.136	0.020	37.42
FH-L-0-e2	5	20.82	0.64	2.65	0.08	28.45	0.39	1.058	0.015	29.49
FH-L-0-e3	5	21.47	1.11	2.23	0.14	45.56	0.94	1.513	5.685	5.69
FH-L-10-a1	15	19.46	0.73	2.66	0.10	44.67	0.72	1.400	0.009	11.53
FH-L-10-a3	15	23.50	0.80	3.15	0.11	60.51	0.88	2.242	0.013	11.89
FH-L-10-b1	15	34.67	1.05	3.75	0.11	66.17	0.86	3.680	0.028	16.31
FH-L-10-b2	15	24.03	1.20	bdl		73.53	1.30	2.153	0.008	6.22
FH-L-10-b3	15	25.47	0.74	3.34	0.11	43.94	0.53	1.896	0.028	32.74
FH-L-10-c1	15	18.67	0.96	3.65	0.15	34.57	0.72	1.197	0.007	6.41
FH-L-10-c3	15	40.43	2.12	0.77	0.13	18.10	0.39	1.107	0.009	15.02
FH-L-10-d1	15	32.13	1.72	3.06	0.18	48.37	1.12	2.525	0.007	3.50
FH-L-10-d2	15	24.87	1.03	2.46	0.11	40.00	0.72	1.607	0.008	8.41
FH-L-10-d3	15	34.53	1.50	bdl		39.92	0.65	1.708	0.012	14.24
FH-L-10-e1	15	21.22	0.81	4.10	0.16	64.69	1.05	2.231	0.009	7.12
FH-L-10-e2	15	17.94	0.54	4.12	0.12	73.45	0.89	2.089	0.017	17.28
FH-L-10-e3	15	22.68	0.68	3.25	0.10	61.09	0.76	2.174	21.955	21.95
FH-L-20-a1	23	24.72	1.04	3.09	0.13	57.77	1.05	2.246	0.008	6.02
FH-L-20-a2	23	26.36	0.75	3.46	0.09	75.95	0.85	3.063	0.034	24.26
FH-L-20-a3	23	32.00	1.25	3.72	0.15	49.83	0.91	2.695	0.010	6.81
FH-L-20-a4	23	21.84	0.69	4.03	0.12	58.38	0.81	2.115	0.015	14.68
FH-L-20-b1	23	12.33	0.71	3.08	0.12	36.43	0.71	0.790	0.006	7.59

Table C.7: Goethite (U-Th)/He ages of pisoliths from depth profile of outcrop Lohn am Randen (d = depth below freshwater limestone layer, gt mass = mass of aliquot based on Fe, stoichiometrically calculated as goethite, ul = layer of paleosol above freshwater limestone, bdl = below detection limit).

Sample Name	d [cm]	age [Ma]	$\pm1\sigma$ [Ma]	U [ppm]	$\pm1\sigma$ [ppm]	Th [ppm]	$\pm1\sigma$ [ppm]	^{4}He [nmol/g]	$\pm1\sigma$ [nmol/g]	Gt Mass [μg]
FH-L-20-b2	23	22.23	0.63	3.55	0.09	63.44	0.72	2.240	0.028	27.47
FH-L-20-b3	23	20.56	0.68	3.30	0.11	60.06	0.85	1.954	0.013	13.38
FH-L-20-c1	23	33.15	1.23	bdl		60.70	0.86	2.577	0.017	14.17
FH-L-20-c2	23	28.57	1.11	0.56	0.14	50.35	0.77	1.929	0.013	13.82
FH-L-20-c3	23	39.26	3.17	bdl		47.40	1.07	1.703	0.007	5.29
FH-L-20-d1	23	32.56	1.05	3.76	0.13	68.32	0.96	3.515	0.019	11.28
FH-L-20-d2	23	29.88	1.04	3.03	0.11	45.21	0.71	2.222	0.013	11.51
FH-L-20-d3	23	27.80	0.83	3.93	0.11	37.03	0.51	1.913	0.020	22.57
FH-L-20-e1	23	11.88	0.35	2.83	0.07	42.54	0.50	0.829	0.014	33.78
FH-L-20-e2	23	14.84	0.88	3.31	0.15	43.61	0.89	1.096	0.006	5.40
FH-L-20-e3	23	15.87	0.50	2.97	0.09	34.87	0.47	0.965	0.013	25.52
FH-L-30-a1	33	10.18	0.46	4.21	0.14	41.50	0.69	0.774	0.007	11.06
FH-L-30-a2	33	11.23	0.58	2.82	0.11	37.25	0.67	0.708	0.007	9.76
FH-L-30-b1	33	17.17	0.54	4.06	0.12	63.52	0.85	1.795	0.014	15.46
FH-L-30-b2	33	18.66	0.77	3.27	0.12	38.70	0.69	1.261	0.008	9.57
FH-L-30-b3	33	25.36	0.98	1.48	0.15	45.42	0.71	1.679	0.012	14.04
FH-L-30-c2	33	30.04	1.00	2.04	0.12	46.04	0.64	2.105	0.020	20.20
FH-L-30-d1	33	24.54	2.00	2.67	0.15	22.66	0.72	1.069	0.006	3.90
FH-L-30-d2	33	19.01	0.57	3.16	0.09	32.57	0.43	1.119	0.016	28.61
FH-L-30-d3	33	20.94	0.73	2.80	0.12	48.89	0.72	1.630	0.012	14.19
FH-L-30-e1	33	21.53	0.78	3.47	0.13	43.62	0.71	1.608	12.136	12.14
FH-L-30-e2	33	22.17	0.85	2.94	0.11	40.78	0.68	1.511	0.009	10.28
FH-L-30-e3	33	18.98	0.66	2.95	0.10	44.08	0.65	1.375	0.011	14.55
FH-L-50-a1	45	21.43	0.66	5.47	0.16	85.24	1.12	3.013	0.018	12.23
FH-L-50-a2	45	26.16	0.72	6.49	0.14	52.85	0.65	2.707	0.030	20.02
FH-L-50-b1	45	23.55	0.68	5.40	0.13	64.03	0.79	2.633	0.024	20.07
FH-L-50-b2	45	17.13	0.63	3.82	0.13	43.28	0.70	1.312	0.009	11.62
FH-L-50-b3	45	35.42	1.05	4.20	0.11	28.05	0.42	2.089	0.023	23.63
FH-L-50-c1	45	15.78	0.52	3.45	0.13	35.35	0.51	1.010	0.012	23.43
FH-L-50-c2	45	44.40	7.98	bdl		29.18	1.21	1.182	0.006	2.96
FH-L-50-c3	45	25.48	1.76	bdl		30.63	0.71	0.993	0.007	7.79
FH-L-50-d1	45	18.34	0.57	3.08	0.10	81.20	1.00	2.214	0.016	15.10
FH-L-50-d2	45	26.26	1.00	3.01	0.13	51.73	0.86	2.169	0.010	8.21
FH-L-50-d3	45	29.34	1.06	1.05	0.13	49.89	0.72	2.043	0.016	16.29
FH-L-50-e1	45	20.46	0.59	3.67	0.10	58.33	0.69	1.935	26.729	26.73
FH-L-50-e3	45	28.12	0.78	2.89	0.07	51.08	0.56	2.280	0.036	35.02
FH-L-70-a1	60	8.18	0.21	9.15	0.20	229.27	2.04	2.811	0.021	16.20
FH-L-70-a2	60	12.74	0.30	16.89	0.22	214.80	1.67	4.683	0.052	24.59
FH-L-70-a3	60	11.46	0.27	15.72	0.21	208.04	1.64	4.032	0.045	24.49

Table C.8: Table of goethite (U-Th)/He ages continued.

Sample Name	d [cm]	age [Ma]	$\pm1\sigma$ [Ma]	U [ppm]	$\pm1\sigma$ [ppm]	Th [ppm]	$\pm1\sigma$ [ppm]	^{4}He [nmol/g]	$\pm1\sigma$ [nmol/g]	Gt Mass [μg]
FH-L-70-b1	60	12.75	0.68	4.88	0.20	69.14	1.29	1.474	0.007	4.62
FH-L-70-b2	60	20.22	1.05	2.69	0.12	40.38	0.83	1.343	0.007	5.91
FH-L-70-b3	60	19.41	0.57	3.60	0.09	35.82	0.46	1.277	0.018	30.55
FH-L-70-c1	60	28.64	1.21	0.19	0.24	80.67	1.30	2.988	0.011	7.32
FH-L-70-c2	60	22.25	0.64	3.50	0.13	75.22	0.83	2.567	0.030	25.29
FH-L-70-c3	60	48.73	1.55	0.45	0.18	152.26	1.81	9.625	0.044	10.03
FH-L-70-d1	60	17.97	0.62	2.95	0.16	51.64	0.73	1.476	0.013	16.76
FH-L-70-d2	60	17.88	0.53	3.65	0.11	67.08	0.80	1.890	0.018	19.93
FH-L-70-d3	60	25.24	1.09	1.32	0.19	45.64	0.79	1.657	0.010	10.62
FH-L-70-e1	60	13.66	0.39	4.77	0.11	44.52	0.55	1.133	0.015	27.32
FH-L-70-e2	60	14.26	0.56	6.13	0.17	20.80	0.41	0.855	0.008	12.76
FH-L-70-e3	60	20.05	0.59	5.77	0.13	18.74	0.30	1.111	0.014	25.27
FH-L-70-g1	60	19.03	0.82	3.06	0.17	87.34	1.50	2.445	5.076	5.08
FH-L-70-g2	60	14.59	0.63	2.98	0.16	103.02	1.66	2.160	5.282	5.28
FH-L-70-g3	60	15.01	0.77	2.90	0.19	95.08	1.73	2.063	3.860	3.86
FH-L-70-g4	60	16.23	1.05	2.82	0.20	70.33	1.51	1.710	3.257	3.26
FH-L-70-g5	60	16.69	0.61	3.13	0.14	103.25	1.50	2.489	7.457	7.46
FH-L-70-g6	60	11.77	0.50	13.48	0.42	79.24	1.44	2.055	4.698	4.70
FH-L-70-g7	60	17.96	0.54	3.16	0.10	65.87	0.80	1.823	21.705	21.70
FH-L-70-g8	60	18.76	0.91	2.92	0.17	67.59	1.28	1.921	4.842	4.84
FH-L-80-a1	75	23.11	0.76	4.07	0.14	88.69	1.24	3.139	0.015	9.56
FH-L-80-a2	75	21.45	0.77	3.77	0.14	85.27	1.29	2.785	0.011	7.52
FH-L-80-b1	75	13.17	0.35	5.20	0.13	84.58	0.82	1.798	0.028	33.68
FH-L-80-b2	75	13.11	0.41	6.69	0.17	73.61	0.97	1.716	0.013	14.21
FH-L-80-b3	75	14.47	0.34	13.50	0.16	156.00	1.21	3.953	0.061	34.38
FH-L-80-c1	75	37.64	1.35	4.30	0.20	63.75	1.05	3.955	0.015	7.70
FH-L-80-c2	75	48.28	2.97	bdl		33.59	0.71	1.824	0.009	8.66
FH-L-80-c3	75	28.03	1.11	3.29	0.15	31.65	0.59	1.637	0.010	10.39
FH-L-80-d1	75	24.73	0.81	3.58	0.12	53.42	0.76	2.173	0.014	13.55
FH-L-80-d2	75	28.92	0.85	2.64	0.08	27.13	0.35	1.420	0.027	42.06
FH-L-80-e1	75	31.03	1.13	2.35	0.09	23.89	0.42	1.347	0.011	15.35
FH-L-80-e2	75	37.56	1.56	bdl		42.89	0.68	2.025	0.014	14.33
FH-L-80-e3	75	29.25	1.98	2.31	0.19	42.38	1.15	1.954	3.130	3.13
FH-L-90-b1	87	41.41	1.68	3.60	0.16	54.50	1.05	3.708	0.011	5.29
FH-L-90-b2	87	19.44	0.65	3.09	0.11	71.70	0.99	2.115	0.013	12.27
FH-L-90-c1	87	33.84	1.35	1.45	0.13	30.70	0.52	1.597	0.013	16.50
FH-L-90-c2	87	28.15	1.28	3.04	0.18	38.28	0.78	1.845	0.008	6.78
FH-L-90-c3	87	29.87	1.12	1.75	0.13	35.25	0.56	1.632	0.014	17.31
FH-L-90-d1	87	16.47	0.63	2.82	0.11	39.96	0.64	1.095	13.548	13.55

Table C.9: Table of goethite (U-Th)/He ages continued.

Sample Name	d [cm]	age [Ma]	$\pm 1\sigma$ [Ma]	U [ppm]	$\pm 1\sigma$ [ppm]	Th [ppm]	$\pm 1\sigma$ [ppm]	^{4}He [nmol/g]	$\pm 1\sigma$ [nmol/g]	Gt Mass [μg]
FH-L-90-d2	87	18.85	0.62	3.93	0.13	40.60	0.60	1.383	0.012	17.35
FH-L-90-d3	87	25.98	1.62	bdl		29.66	0.63	0.959	0.007	9.63
FH-L-90-e1	87	19.86	0.54	2.54	0.07	70.92	0.71	2.077	0.032	33.86
FH-L-90-e2	87	22.11	0.86	3.27	0.14	68.32	1.11	2.328	0.009	6.76
FH-L-90-e3	87	16.67	0.61	3.41	0.13	78.63	1.15	1.988	0.010	8.56
FH-L-120-a1	116	31.42	0.80	4.54	0.08	46.26	0.47	2.645	0.064	54.12
FH-L-120-a2	116	45.07	2.07	0.81	0.14	27.83	0.53	1.806	0.012	13.54
FH-L-120-b1	116	47.08	1.49	3.32	0.11	64.23	0.89	4.740	0.029	13.50
FH-L-120-b2	116	24.14	0.85	3.01	0.12	64.20	0.96	2.380	0.012	9.66
FH-L-120-b3	116	45.53	1.59	3.03	0.12	57.56	0.92	4.119	0.018	9.18
FH-L-120-c1	116	25.65	1.12	bdl		70.51	1.10	2.142	0.011	9.09
FH-L-120-c2	116	37.71	2.39	bdl		66.84	1.30	2.462	0.008	5.28
FH-L-120-c3	116	23.62	0.88	3.03	0.13	76.77	1.20	2.711	0.010	6.99
FH-L-120-d1	116	24.61	0.64	3.17	0.07	70.64	0.65	2.650	0.051	42.91
FH-L-120-d2	116	30.96	0.90	1.65	0.09	74.11	0.80	3.217	0.041	28.15
FH-L-120-d3	116	27.35	0.72	4.24	0.09	61.34	0.62	2.779	0.047	37.35
FH-L-120-e1	116	36.91	0.93	5.82	0.09	21.88	0.28	2.204	0.056	56.75
FH-L-120-e2	116	42.16	1.43	5.77	0.17	14.92	0.34	2.133	0.013	12.05
FH-L-120-e3	116	18.80	0.92	8.50	0.31	42.99	0.97	1.904	0.007	4.19
FH-L-120-f1	116	17.05	0.69	3.03	0.13	59.36	0.97	1.576	0.008	8.46
FH-L-120-f2	116	17.68	1.35	3.23	0.20	52.37	1.32	1.496	0.006	2.93
FH-L-120-f3	116	16.96	0.70	2.71	0.12	58.50	0.97	1.520	0.008	8.16
FH-L-120-f4	116	15.51	1.96	2.54	0.26	63.89	1.98	1.482	0.006	1.59
FH-L-120-f5	116	18.23	0.96	2.91	0.16	59.30	1.18	1.672	0.007	4.68
FH-L-120-f7	116	21.39	1.13	2.23	0.12	44.33	0.92	1.473	0.007	5.50
FH-L-120-f8	116	23.46	0.81	2.20	0.09	52.36	0.77	1.854	0.013	13.86
FH-L-120-f9	116	21.54	0.79	2.20	0.09	40.00	0.63	1.361	0.011	14.32
FH-L-120-f10	116	18.12	0.61	2.23	0.08	44.36	0.62	1.249	0.012	18.97
FH-L-120-f11	116	23.56	1.35	2.67	0.14	36.44	0.86	1.441	0.007	4.94
FH-L-120-f12	116	20.32	0.96	2.37	0.11	38.88	0.76	1.273	0.007	7.59
FH-L-120-f13	116	21.60	0.81	2.25	0.09	37.38	0.61	1.298	0.010	13.53
FH-L-120-f14	116	22.61	0.91	2.32	0.10	37.20	0.65	1.362	0.009	10.87
FH-L-120-f16	116	28.02	1.68	1.65	0.15	64.46	1.50	2.564	0.007	2.88
FH-L-120-f17	116	28.25	1.34	1.83	0.11	54.91	1.08	2.268	0.008	5.16
FH-L-120-f18	116	28.19	1.12	2.76	0.13	54.93	0.96	2.406	0.010	7.35
FH-L-120-f20	116	28.21	1.23	1.86	0.11	53.79	0.99	2.228	0.009	6.34
FH-L-120-f21	116	40.54	1.65	1.13	0.06	24.27	0.45	1.509	0.011	13.86
FH-L-120-f22	116	35.83	1.18	1.08	0.04	23.84	0.34	1.305	0.021	34.21
FH-L-120-f23	116	36.76	2.14	1.43	0.09	24.76	0.64	1.452	0.007	5.85

Table C.10: Table of goethite (U-Th)/He ages continued.

Sample Name	d [cm]	age [Ma]	$\pm1\sigma$ [Ma]	U [ppm]	$\pm1\sigma$ [ppm]	Th [ppm]	$\pm1\sigma$ [ppm]	^{4}He [nmol/g]	$\pm1\sigma$ [nmol/g]	Gt Mass [μg]
FH-L-170-a1	164	23.27	0.78	2.12	0.07	43.36	0.62	1.567	0.014	17.98
FH-L-170-a2	164	24.42	0.95	1.73	0.07	37.52	0.63	1.432	0.010	12.13
FH-L-170-a3	164	23.39	0.67	2.21	0.06	60.97	0.68	2.141	0.030	30.60
FH-L-170-b2	164	19.82	0.74	1.48	0.05	24.14	0.39	0.778	0.009	21.32
FH-L-170-b3	164	24.30	0.75	1.77	0.05	32.86	0.43	1.259	0.020	33.50
FH-L-170-c2	164	28.22	1.78	bdl		37.99	0.74	1.107	0.007	9.21
FH-L-170-d1	164	21.67	0.69	1.50	0.05	25.32	0.34	0.880	0.015	34.00
FH-L-170-d2	164	21.81	1.14	1.23	0.10	25.67	0.53	0.862	0.007	10.04
FH-L-170-d3	164	19.05	0.78	1.71	0.08	35.54	0.59	1.044	0.008	12.34
FH-L-170-e2	164	14.87	1.02	2.99	0.16	52.27	1.12	1.236	0.006	3.91
FH-L-170-e3	164	15.63	0.82	3.06	0.13	34.68	0.68	0.953	0.007	7.53
FH-L-250-a1	268	22.93	0.75	3.83	0.13	69.10	0.98	2.515	0.014	11.63
FH-L-250-a2	268	16.99	0.76	2.71	0.13	75.91	1.30	1.903	0.008	5.54
FH-L-250-b1	268	18.27	0.57	5.45	0.16	77.05	1.03	2.349	0.015	12.68
FH-L-250-b2	268	27.27	1.25	3.55	0.16	48.74	1.00	2.233	0.008	5.01
FH-L-250-b3	268	19.13	1.15	2.79	0.14	48.86	1.07	1.490	0.007	4.20
FH-L-250-c1	268	16.52	0.41	4.36	0.08	80.77	0.67	2.099	0.052	54.81
FH-L-250-c2	268	42.85	2.70	bdl		87.26	1.71	3.661	0.009	3.98
FH-L-250-c3	268	37.06	1.93	bdl		91.75	1.61	3.635	0.010	5.05
FH-L-250-d1	268	35.66	0.98	3.59	0.08	38.25	0.45	2.445	0.042	38.08
FH-L-250-d2	268	49.05	2.09	1.30	0.16	32.43	0.59	2.386	0.015	12.97
FH-L-250-d3	268	42.13	1.39	2.68	0.13	35.06	0.52	2.508	0.025	21.93
FH-L-250-e2	268	25.33	0.76	2.19	0.07	46.81	0.57	1.820	0.022	26.27
FH-L-300-a1	339	19.90	1.06	2.08	0.12	58.57	1.16	1.726	0.007	4.55
FH-L-300-a2	339	20.86	0.84	1.76	0.08	57.68	0.94	1.742	0.009	8.53
FH-L-300-a3	339	18.73	0.71	2.04	0.08	56.19	0.86	1.558	0.009	10.68
FH-L-300-b1	339	23.66	0.76	3.78	0.13	110.89	1.45	3.855	0.018	9.54
FH-L-300-b2	339	17.14	0.56	2.83	0.10	90.28	1.16	2.272	0.014	12.41
FH-L-300-b4	339	26.63	0.98	2.47	0.10	46.12	0.75	1.935	0.011	10.88
FH-L-300-b5	339	12.43	0.67	3.59	0.17	95.45	1.70	1.766	0.007	3.86
FH-L-300-b6	339	13.61	1.05	2.92	0.18	79.28	1.73	1.603	0.006	2.59
FH-L-300-c2	339	26.42	1.07	3.18	0.14	58.41	1.02	2.432	0.009	6.24
FH-L-300-c3	339	14.12	1.44	1.96	0.13	39.49	1.02	0.865	0.006	3.39
FH-L-300-d1	339	17.80	0.70	5.03	0.19	33.28	0.61	1.245	0.008	10.36
FH-L-300-d2	339	16.18	0.41	5.19	0.09	32.72	0.36	1.134	0.027	52.73
FH-L-300-d3	339	16.52	0.48	4.45	0.10	28.40	0.39	1.000	32.529	32.53
FH-L-300-e1	339	18.11	0.53	6.50	0.16	61.65	0.79	2.070	0.017	17.07
FH-L-300-e2	339	17.91	0.44	6.12	0.10	65.77	0.60	2.104	0.046	48.81
FH-L-300-e3	339	12.06	0.59	6.16	0.25	89.37	1.54	1.784	0.007	4.31

Table C.11: Table of goethite (U-Th)/He ages continued.